Max-log demapper architecture design for DVB-T2 rotated QAM constellations

Jianxiao Yang, Meng Li, Min Li, Charbel Abdel Nour, Catherine Douillard, Benoit Geller

Max-Log Demapper Architecture Design for DVB-T2 Rotated QAM Constellations

Jianxiao YANG [1], Meng LI [2], Min LI [3],

Charbel ABDEL NOUR [4], Catherine DOUILLARD [4], and Benoit GELLER [1],

***Abstract* — Rotated and cyclic-Q delayed (RCQD) quadrature amplitude modulation (QAM) improve DVB-T2 system performance over highly time-frequency selective channels. However, when compared with conventional QAM demapper, the RCQD demapper requires a higher computational complexity. In this paper, a complexity-reduced max-log demapper is derived and implemented over a FPGA platform. The proposed demapper allows to find the maximum likelihood (ML) point with a search spanning only $\sqrt{M}$ signal constellation points and guarantees to obtain the same log-likelihood ratio (LLR) metrics as the optimum max-log soft decision demapper while spanning at most $2\sqrt{M}$ signal constellation points. The optimized hardware implementation introduces only a slight performance loss compared to the floating-point full complexity max-log performance.**

***Index Terms* — DVB-T2, Rotated and Cyclic Q Delayed (RCQD) Constellations, Log-Likelihood Ratio (LLR), Max-Log Demapper.**

I. INTRODUCTION

DVB-T2 standard [1] improves system performance over highly attenuated or erased time-frequency selective channels when compared to DVB-T [2]. One of the most important reasons for this improvement is the rotated and cyclic Q delayed (RCQD) quadrature amplitude modulation (QAM) [3],[4] which introduces signal space diversity (SSD). This SSD is implemented by two key steps: first, both the in-phase (I) component and the quadrature (Q) components contain full symbol information created by some constellation rotation, and the second step is that the I and Q components are transmitted over independently fading OFDM subcarriers thanks to the insertion of cyclic delay between the I and Q components.

However, SSD requires the corresponding optimum demapper to be performed over the 2D constellation plane [7] instead of two independent 1D demapping for conventional non-rotated constellations. For high order constellations such as 64-QAM or 256-QAM, the computational complexity of a 2D-DEM has a non-negligible impact on receiver design. There have been many studies tackling this complexity problem. The decorrelation based method such as zero forcing (ZF) or minimum mean square error (MMSE) demapper [8] can achieve a low complexity but introduces a huge performance loss especially over channels with severe conditions such as deep fades or erasures. Various simplified 2D demappers [9]-[14] were also proposed to balance a trade-off between complexity and performance. A simplified method was first presented in [9]-[11] based on the decomposition of signal space into sub-regions, each approximately corresponding to one quadrant of the QAM constellation; the demapping operations performed over one sub-region reduces by 61% and by 69% the computational complexity of a 64-QAM and of a 256-QAM respectively. A similar approach was presented in [12] by adaptively adjusting the sub-region with the signal-to-noise ratio (SNR). A so-called sub-region per dimension demapping (PER-DEM) method was provided in [13] with an exploration space down to $2\sqrt{M}$ for a RCQD *M*-QAM. This method starts by dividing the constellation space into regions limited by parallel lines along the imaginary axis; then it computes the distance to the received observation only with respect to points within the two regions closest to the received observation. Another method with sub-region decomposition was proposed in [14] based on the observation of 2D LLR contours as a function of I/Q Rayleigh fading channel attenuations. Although this method explores only $\sqrt{M}$ points, no decoded performance was given so that the associated performance penalty was not reported. For all these 2D sub-region based methods, there is always a possibility of missing the closest constellation point to the channel observation due to the unbalanced (or different) I and Q channel attenuations. Therefore, all these methods are clearly not optimum.

This paper proposes an exact max-log soft demapper with reduced complexity thanks to the proposed simplified detection algorithm and its corresponding hardware. The proposed exact max-log method is able to find the closest point to the received observation *i.e.*, the optimum hard decision by exploring, at most, a space of $\sqrt{M}$ points. It also guarantees to perform exact max-log LLR computations *i.e.*, soft decision for all the bits of a symbol by exploring at most a space of $2\sqrt{M}-1$ points. Finally, this paper also compares objectively the C-floating point algorithm with a VHDL implementation which validates the proposed approach.

The remainder of the paper is organized as follows; system model and the conventional soft demapping process are

Manuscript received April 20, 2015. This work was supported in part by the ANR Greencocom project.

[1] Jianxiao YANG, and Benoit GELLER are with Department U2IS of ENSTA-ParisTech, UPSA, 828 Boulevard des Maréchaux, 91120, Palaiseau, France (e-mail: jianxiao.yang, benoit.geller @ensta-paristech.fr);

[2] Meng LI is with green radio group of IMEC, Kapeldreef 75, 3001 Heverlee, Belgium (e-mail: meng.li@imec.be);

[3] Min LI is with NXP Semiconductors, Interleuvenlaan 80, 3001, Leuven Belgium (email: min.li@nxp.com);

[4] Charbel ABDEL NOUR and Catherine DOUILLARD are with Lab-STICC UMR CNRS 6285, and they are also with ELEC Dépt. Electronique, Institut Mines Télécom - Télécom Bretagne, CS 83818, 29238 BREST cedex 3, France (e-mail: charbel.abdelnour, catherine.douillard @telecom-bretagne.eu).

introduced in section II. The derivation and the architecture design of the proposed complexity-reduced exact max-log demapper are detailed in section III. Logic synthesis results and the evaluated performance are given in section IV. Finally, Section V concludes the paper.

II. System Model for RCQD Constellations

A. Rotated and Cyclic-Q Delayed Constellations

A conventional square M -QAM constellation can be regarded as a signal with two independent $\sqrt{M}$ -PAM components and takes values from the following $\mathbf{S}_c$ set:

$$\mathbf{S}_c = \left\{ s = s_I + j s_Q \,|\, s_I, s_Q \in \mathbf{A}_c \right\}, \tag{1}$$

where $\mathbf{A}_c$ is defined as:

$$\mathbf{A}_c = \left\{ s_x \,\middle|\, s_x = \frac{2}{\sigma_s}\left(-\frac{1}{2}\left(\sqrt{M}-1\right) + p_x \right), p_x \in \mathbf{I}_c \right\}, \tag{2}$$

where $x = I$ or Q , $\mathbf{I}_c = \left\{0,1,\cdots,\sqrt{M}-1\right\}$ is an integer set and σ_s is a QAM normalization factor (*e.g.*, for 256-QAM $\sigma_s = \sqrt{170}$).

In order to obtain a RCQD constellation, the conventional square symbol is first rotated by an angle θ to obtain a rotated symbol $z = s\exp(j\theta)$. Then the imaginary part of z is delayed by one symbol period to build the symbol x such that $x = \mathrm{Re}(z) + j\,\mathrm{Im}(z')$. Consequently, the real and imaginary parts of symbol z are transmitted over two different independent and identically distributed fading events. Equivalently, for orthogonal frequency-division multiplexing (OFDM)-based systems such as DVB-T2, these parts are transmitted over two sufficiently spaced subcarriers of an OFDM symbol, therefore doubling the diversity order.

Let $h_I \geq 0$ and $h_Q \geq 0$ denote Rayleigh distributed fading coefficients that affect the two subcarriers where symbol z has been transmitted. The observed symbol $y = y_I + j y_Q$ received by the demapper can be expressed as:

$$\begin{aligned} y_I + j y_Q &= \left(h_I z_I + n_I\right) + j\left(h_Q z_Q + n_Q\right) \\ &= \left[h_I\left(s_I\cos\theta - s_Q\sin\theta\right) + n_I \right] \\ &\quad + j\left[h_Q\left(s_I\sin\theta + s_Q\cos\theta\right) + n_Q \right], \end{aligned} \tag{3}$$

where $n = n_I + j n_Q$ represents a zero-mean circularly symmetric complex Gaussian noise term with variance σ_n^2. Thus, equation (3) can be rewritten as:

$$\begin{aligned} \mathbf{y} = \mathbf{hs} + \mathbf{n} &= \begin{pmatrix} \mathbf{h}_1 & \mathbf{h}_2 \end{pmatrix}\mathbf{s} + \mathbf{n} = \mathbf{h}_1 s_I + \mathbf{h}_2 s_Q + \mathbf{n} \\ &= \begin{pmatrix} h_I\cos\theta & -h_I\sin\theta \\ h_Q\sin\theta & h_Q\cos\theta \end{pmatrix}\begin{pmatrix} s_I \\ s_Q \end{pmatrix} + \begin{pmatrix} n_I \\ n_Q \end{pmatrix}, \end{aligned} \tag{4}$$

where $\mathbf{y} = \begin{pmatrix} y_I \\ y_Q \end{pmatrix}$, $\mathbf{h} = \begin{pmatrix} \mathbf{h}_1 & \mathbf{h}_2 \end{pmatrix}$, $\mathbf{h}_1 = \begin{pmatrix} h_{1,1} \\ h_{2,1} \end{pmatrix} = \begin{pmatrix} h_I\cos\theta \\ h_Q\sin\theta \end{pmatrix}$, $\mathbf{h}_2 = \begin{pmatrix} h_{1,2} \\ h_{2,2} \end{pmatrix} = \begin{pmatrix} -h_I\sin\theta \\ h_Q\cos\theta \end{pmatrix}$, $\mathbf{s} = \begin{pmatrix} s_I \\ s_Q \end{pmatrix}$ and $\mathbf{n} = \begin{pmatrix} n_I \\ n_Q \end{pmatrix}$.

B. Soft-Demapping Process

The RCQD constellation breaks the independency between the I and Q components of the signals in the signal space plane. Indeed, both I and Q components contribute to the estimation of the log likelihood $\mathrm{LLR}(b_i)$ of each transmitted bit b_i with $i = 0,1,\cdots,\log_2 M - 1$. Therefore the accurate LLR computation requires an exploration of a signal space containing all the possible M complex-valued constellation points:

$$\begin{aligned} \mathrm{LLR}(b_i) = &\ln\left(\sum_{\mathbf{s}\in\mathbf{S}_c(b_i=0)} \exp\left(-\frac{1}{\sigma_n^2}\left\|\mathbf{y}-\mathbf{hs}\right\|^2 \right) \right) \\ &- \ln\left(\sum_{\mathbf{s}\in\mathbf{S}_c(b_i=1)} \exp\left(-\frac{1}{\sigma_n^2}\left\|\mathbf{y}-\mathbf{hs}\right\|^2 \right) \right), \end{aligned} \tag{5}$$

where $\mathbf{S}_c(b_i = b)$ denotes the subset of $\mathbf{S}_c$ that contains all constellation points associated with $b_i = b$ and $b = \{0,1\}$.

A soft demapping solution with a negligible loss [7] can be obtained by applying the max-log approximation over (5):

$$\begin{aligned} \mathrm{LLR}(b_i) &\approx \frac{1}{\sigma_n^2}\left(\max_{\mathbf{s}\in\mathbf{S}_c(b_i=0)} \left\{ -\left\|\mathbf{y}-\mathbf{hs}\right\|^2 \right\} - \max_{\mathbf{s}\in\mathbf{S}_c(b_i=1)} \left\{ -\left\|\mathbf{y}-\mathbf{hs}\right\|^2 \right\} \right) \\ &= -\left(\gamma_{\min}(b_i = 0) - \gamma_{\min}(b_i = 1) \right), \end{aligned} \tag{6}$$

where $\gamma_{\min}(b_i = b) = \frac{1}{\sigma_n^2}\min_{\mathbf{s}\in\mathbf{S}_c(b_i=b)}\left\{ \left\|\mathbf{y}-\mathbf{hs}\right\|^2 \right\}$ represents the log-likelihood metric of $b_i = b$. Although (6) simplifies the computational complexity, it still implies to explore the M complex-valued constellation points. However, it should be noted from (6) that the LLR computation becomes an evaluation of the Euclidean distance between the observation vector $\mathbf{y}$ and the two closest points with bits b_i taking values 0 and 1. Then if there exists such an algorithm that these two closest points can be found for each bit b_i without exploring the whole constellation plane, the max-log demapper can be achieved with reduced complexity.

III. Complexity-Reduced Max-Log Demapper Design

A. The Derivation of the Proposed Algorithm

For a given constellation component $s_Q \in \mathbf{A}_c$ (*resp.* $s_I \in \mathbf{A}_c$) in (4), the equivalent observation $\mathbf{r}_I$ (*resp.* $\mathbf{r}_Q$) of the other component s_I (*resp.* s_Q) becomes:

$$\begin{cases} \mathbf{r}_I \triangleq \mathbf{y} - \mathbf{h}_2 s_Q = \mathbf{h}_1 s_I + \mathbf{n}, \\ \mathbf{r}_Q \triangleq \mathbf{y} - \mathbf{h}_1 s_I = \mathbf{h}_2 s_Q + \mathbf{n}. \end{cases} \tag{7}$$

Then the Euclidean distance between the equivalent observation and the component $\left\|\mathbf{r}_I - \mathbf{h}_1 s_I\right\|^2$ can be expressed as:

$$\begin{aligned} \left\|\mathbf{r}_I - \mathbf{h}_1 s_I\right\|^2 &= \left(r_{I,1} - h_{1,1}s_I\right)^2 + \left(r_{I,2} - h_{2,1}s_I\right)^2 \\ &= \left(h_{1,1}^2 + h_{2,1}^2\right)\left(s_I - \bar{v}\right)^2 + \frac{\left(h_{1,1}r_{I,2} - h_{2,1}r_{I,1}\right)^2}{h_{1,1}^2 + h_{2,1}^2} \end{aligned} \tag{8}$$

where $\bar{v} = \frac{h_{1,1}r_{I,1} + h_{2,1}r_{I,2}}{h_{1,1}^2 + h_{2,1}^2}$, so that the closest candidate point $\left(s_{I,\min}, s_Q\right)$ based on a given s_Q can be computed by rounding $\bar{v}$ to its nearest value s_x in $\mathbf{A}_c$ (see (2)). It should be noted from (8) that the closest point $\left(s_{I,\min}, s_Q\right)$ (*resp.* $\left(s_I, s_{Q,\min}\right)$) to the observation $\mathbf{r}_I$ (*resp.* $\mathbf{r}_Q$) can be computed without being compared with other Euclidean distance terms.

Therefore, the essential idea of this 2-D global minimization problem can be simplified as follows: for each given value $s_Q \in \mathbf{A}_c$ (*resp.* $s_I \in \mathbf{A}_c$), search the closest point $s_{I,\min}$ (*resp.* $s_{Q,\min}$) to the equivalent observation solution $\mathbf{r}_I$ (*resp.* $\mathbf{r}_Q$) in (7) with the known equivalent channel response $\mathbf{h}_1$ (*resp.* $\mathbf{h}_2$) by rounding $\bar{v}$. The global optimum solution must then belong to one of the $\sqrt{M}$ local optimum solutions $(s_{I,\min}, s_Q)$ (*resp.* $(s_I, s_{Q,\min})$).

It should also be noted that the candidate value $\{s_{I,\min}\}$, $\{s_{Q,\min}\}$ and the Euclidean distance term $\{\|\mathbf{y}-\mathbf{hs}\|^2\}$ requires the implementation of many parallel dividers, multipliers and comparators. In order to further reduce the computational complexity, the following transformations over (4) are proposed.

First, both sides of (4) are divided by the factor σ_n and are extended as below:

$$\begin{aligned}\frac{1}{\sigma_n}\mathbf{y} &= \frac{1}{\sigma_n}\begin{pmatrix} h_I\cos\theta & -h_I\sin\theta \\ h_Q\sin\theta & h_Q\cos\theta \end{pmatrix}\begin{pmatrix} s_I \\ s_Q \end{pmatrix}+\frac{1}{\sigma_n}\begin{pmatrix} n_I \\ n_Q \end{pmatrix} \\ &= \frac{1}{\sigma_n}\begin{pmatrix} h_I\cos\theta & -h_I\sin\theta \\ h_Q\sin\theta & h_Q\cos\theta \end{pmatrix}\begin{pmatrix} \frac{2}{\sigma_s}\left(-\frac{1}{2}\left(\sqrt{M}-1\right)+p_I\right) \\ \frac{2}{\sigma_s}\left(-\frac{1}{2}\left(\sqrt{M}-1\right)+p_Q\right) \end{pmatrix}+\frac{1}{\sigma_n}\begin{pmatrix} n_I \\ n_Q \end{pmatrix} \\ &= \frac{2}{\sigma_n\sigma_s}\begin{pmatrix} h_I\cos\theta & -h_I\sin\theta \\ h_Q\sin\theta & h_Q\cos\theta \end{pmatrix}\begin{pmatrix} p_I \\ p_Q \end{pmatrix}+\frac{1}{\sigma_n}\begin{pmatrix} n_I \\ n_Q \end{pmatrix} \\ &\quad -\frac{1}{\sigma_n\sigma_s}\left(\sqrt{M}-1\right)\begin{pmatrix} h_I\left(\cos\theta-\sin\theta\right) \\ h_Q\left(\sin\theta+\cos\theta\right) \end{pmatrix},\end{aligned} \tag{9}$$

where p_I (*resp.* p_Q) is defined in (2) and represents the equivalent constellation component of s_I (*resp.* s_Q)

Second, if the last constant term in (9) is moved to the left-hand side, an equivalent observation model $\tilde{\mathbf{y}}$ can be derived as:

$$\begin{aligned}\tilde{\mathbf{y}} &\triangleq \begin{pmatrix} \tilde{y}_I \\ \tilde{y}_Q \end{pmatrix} \triangleq \frac{1}{\sigma_n}\mathbf{y}+\frac{1}{\sigma_n\sigma_s}\left(\sqrt{M}-1\right)\begin{pmatrix} h_I\left(\cos\theta-\sin\theta\right) \\ h_Q\left(\sin\theta+\cos\theta\right) \end{pmatrix} \\ &= \frac{1}{\sigma_n}(\mathbf{hs}+\mathbf{n})+\frac{1}{\sigma_n\sigma_s}\left(\sqrt{M}-1\right)\begin{pmatrix} h_I\left(\cos\theta-\sin\theta\right) \\ h_Q\left(\sin\theta+\cos\theta\right) \end{pmatrix} \\ &= \frac{2}{\sigma_n\sigma_s}\begin{pmatrix} h_I\cos\theta & -h_I\sin\theta \\ h_Q\sin\theta & h_Q\cos\theta \end{pmatrix}\begin{pmatrix} p_I \\ p_Q \end{pmatrix}+\frac{1}{\sigma_n}\begin{pmatrix} n_I \\ n_Q \end{pmatrix} \\ &= \begin{pmatrix} \tilde{h}_{1,1} & \tilde{h}_{1,2} \\ \tilde{h}_{2,1} & \tilde{h}_{2,2} \end{pmatrix}\begin{pmatrix} p_I \\ p_Q \end{pmatrix}+\begin{pmatrix} \tilde{n}_I \\ \tilde{n}_Q \end{pmatrix} \triangleq \tilde{\mathbf{h}}\mathbf{p}+\tilde{\mathbf{n}},\end{aligned} \tag{10}$$

where the equivalent observation terms $\tilde{y}_I$, $\tilde{y}_Q$, the equivalent channel response terms $\tilde{h}_{1,1}$, $\tilde{h}_{2,1}$, $\tilde{h}_{1,2}$, $\tilde{h}_{2,2}$, and the equivalent noise terms $\tilde{n}_I$, $\tilde{n}_Q$ are as follows:

$$\tilde{y}_I = \frac{1}{\sigma_n}\left(y_I+\frac{1}{\sigma_s}\left(\sqrt{M}-1\right)\left(\cos\theta-\sin\theta\right)h_I\right), \tag{11}$$

$$\tilde{y}_Q = \frac{1}{\sigma_n}\left(y_Q+\frac{1}{\sigma_s}\left(\sqrt{M}-1\right)\left(\sin\theta+\cos\theta\right)h_Q\right), \tag{12}$$

$$\tilde{h}_{1,1} = \frac{1}{\sigma_n}\frac{2\cos\theta}{\sigma_s}h_I, \tag{13}$$

$$\tilde{h}_{2,1} = \frac{1}{\sigma_n}\frac{2\sin\theta}{\sigma_s}h_Q, \tag{14}$$

$$\tilde{h}_{1,2} = -\frac{1}{\sigma_n}\frac{2\sin\theta}{\sigma_s}h_I, \tag{15}$$

$$\tilde{h}_{2,2} = \frac{1}{\sigma_n}\frac{2\cos\theta}{\sigma_s}h_Q, \tag{16}$$

$$\tilde{n}_I = \frac{1}{\sigma_n}n_I, \tag{17}$$

$$\tilde{n}_Q = \frac{1}{\sigma_n}n_Q, \tag{18}$$

$$\tilde{\mathbf{h}} \triangleq \begin{pmatrix} \tilde{h}_{1,1} & \tilde{h}_{1,2} \\ \tilde{h}_{2,1} & \tilde{h}_{2,2} \end{pmatrix}, \tag{19}$$

$$\tilde{\mathbf{n}} \triangleq \begin{pmatrix} \tilde{n}_I \\ \tilde{n}_Q \end{pmatrix}, \tag{20}$$

$$\tilde{\mathbf{p}} \triangleq \begin{pmatrix} \tilde{p}_I \\ \tilde{p}_Q \end{pmatrix},. \tag{21}$$

Finally, based on the results of (8), the local optimum solution $p_{I,\min}$ (*resp.* p_Q) with the given value $p_Q \in \mathbf{I}_c$ (*resp.* $p_I \in \mathbf{I}_c$) can be derived as well:

$$\begin{aligned}p_{I,\min} &= \arg\min_{p_I\in\mathbf{I}_c}\left|\frac{\tilde{h}_{1,1}\left(\tilde{y}_I-\tilde{h}_{1,2}p_Q\right)+\tilde{h}_{2,1}\left(\tilde{y}_Q-\tilde{h}_{2,2}p_Q\right)}{\tilde{h}_{1,1}^2+\tilde{h}_{2,1}^2}-p_I\right| \\ &= \text{round}\left(\frac{\tilde{h}_{1,1}\tilde{y}_I+\tilde{h}_{2,1}\tilde{y}_Q}{\tilde{h}_{1,1}^2+\tilde{h}_{2,1}^2}-\frac{\tilde{h}_{1,1}\tilde{h}_{1,2}+\tilde{h}_{2,1}\tilde{h}_{2,2}}{\tilde{h}_{1,1}^2+\tilde{h}_{2,1}^2}p_Q\right) \\ &= \text{round}\left(\tilde{r}_I+\tilde{c}_Q p_Q\right),\end{aligned} \tag{22}$$

$$\begin{aligned}p_{Q,\min} &= \arg\min_{p_Q\in\mathbf{I}_c}\left|\frac{\tilde{h}_{1,2}\left(\tilde{y}_I-\tilde{h}_{1,1}p_I\right)+\tilde{h}_{2,2}\left(\tilde{y}_Q-\tilde{h}_{2,1}p_I\right)}{\tilde{h}_{1,2}^2+\tilde{h}_{2,2}^2}-p_Q\right| \\ &= \text{round}\left(\frac{\tilde{h}_{1,2}\tilde{y}_I+\tilde{h}_{2,2}\tilde{y}_Q}{\tilde{h}_{1,2}^2+\tilde{h}_{2,2}^2}-\frac{\tilde{h}_{1,2}\tilde{h}_{1,1}+\tilde{h}_{2,2}\tilde{h}_{2,1}}{\tilde{h}_{1,2}^2+\tilde{h}_{2,2}^2}p_I\right) \\ &= \text{round}\left(\tilde{r}_Q+\tilde{c}_I p_I\right),\end{aligned} \tag{23}$$

where $\tilde{r}_I$, $\tilde{c}_Q$, $\tilde{r}_Q$ and $\tilde{c}_I$ are:

$$\tilde{r}_I = \frac{\tilde{h}_{1,1}\tilde{y}_I+\tilde{h}_{2,1}\tilde{y}_Q}{\tilde{h}_{1,1}^2+\tilde{h}_{2,1}^2}, \tag{24}$$

$$\tilde{c}_Q = -\frac{\tilde{h}_{1,1}\tilde{h}_{1,2}+\tilde{h}_{2,1}\tilde{h}_{2,2}}{\tilde{h}_{1,1}^2+\tilde{h}_{2,1}^2}, \tag{25}$$

$$\tilde{r}_Q = \frac{\tilde{h}_{1,2}\tilde{y}_I+\tilde{h}_{2,2}\tilde{y}_Q}{\tilde{h}_{1,2}^2+\tilde{h}_{2,2}^2}, \tag{26}$$

$$\tilde{c}_I = -\frac{\tilde{h}_{1,2}\tilde{h}_{1,1}+\tilde{h}_{2,2}\tilde{h}_{2,1}}{\tilde{h}_{1,2}^2+\tilde{h}_{2,2}^2}. \tag{27}$$

Therefore, the corresponding local minimum distance with the corresponding value of $p_Q \in \mathbf{I}_c$ (or $p_I \in \mathbf{I}_c$) can be computed as:

$$\gamma\left(p_{I,\min}, p_Q\right) = \left(\tilde{y}_I-\tilde{h}_{1,1}p_{I,\min}-\tilde{h}_{1,2}p_Q\right)^2+\left(\tilde{y}_Q-\tilde{h}_{2,1}p_{I,\min}-\tilde{h}_{2,2}p_Q\right)^2, \tag{28}$$

$$\gamma\left(p_I, p_{Q,\min}\right) = \left(\tilde{y}_I-\tilde{h}_{1,1}p_I-\tilde{h}_{1,2}p_{Q,\min}\right)^2+\left(\tilde{y}_Q-\tilde{h}_{2,1}p_I-\tilde{h}_{2,2}p_{Q,\min}\right)^2. \tag{29}$$

Thanks to these previous derivations, the optimization of the proposed complexity-reduced exact max-log demapper is achieved at the algorithm level; we summarize it as follows:

The complexity-reduced max-log (CRML) demapping algorithm:

0. Initialize the metric terms $\gamma_{\min}(b_i = b) = -\infty$ for $i = 0,1,\cdots,\log_2 M - 1$ and $b_i = 0,1$;

1. Compute the various factor terms of the equivalent demapping model:
   a. Compute the terms $\tilde{y}_I$, $\tilde{y}_Q$, $\tilde{h}_{1,1}$, $\tilde{h}_{2,1}$, $\tilde{h}_{1,2}$ and $\tilde{h}_{2,2}$ for the equivalent observation model in (10) by using (11)-(16);
   b. Compute the terms $\tilde{r}_I$, $\tilde{c}_Q$, $\tilde{r}_Q$ and $\tilde{c}_I$ for the equivalent Euclidean distance terms of (22) and (23) by using (24)-(27);
2. For each $p_I = 0,1,\cdots,\sqrt{M}-1$, perform the following steps:

a. Compute $p_{Q,\min}$ by (23);

b. Compute the metric term $\gamma\left(p_I, p_{Q,\min}\right)$ by (29);

c. Update the bit metric terms for $\gamma_{\min}\left(b_i = b_i\left(p_I, p_{Q,\min}\right)\right)$ for $i = 0,1,\cdots,\log_2 M - 1$ and for $b = 0,1$ according to the current symbol $\left(p_I, p_{Q,\min}\right)$:

{

If $\gamma_{\min}\left(b_i = b_i\left(p_I, p_{Q,\min}\right)\right) > \gamma\left(p_I, p_{Q,\min}\right)$,

then $\gamma_{\min}\left(b_i = b_i\left(p_I, p_{Q,\min}\right)\right) = \gamma\left(p_I, p_{Q,\min}\right)$

};

3. For each b_i with $p_Q = 0,1,\cdots,\sqrt{M} - 1$, perform the following steps:

a. Compute $p_{I,\min}$ by (22);

b. Compute the metric term $\gamma\left(p_{I,\min}, p_Q\right)$ by (28);

c. Update the bit metric terms for $\gamma_{\min}\left(b_i = b_i\left(p_{I,\min}, p_Q\right)\right)$ for $i = 0,1,\cdots,\log_2 M - 1$ and for $b = 0,1$ according to the current symbol $\left(p_{I,\min}, p_Q\right)$:

{

If $\gamma_{\min}\left(b_i = b_i\left(p_{I,\min}, p_Q\right)\right) > \gamma\left(p_{I,\min}, p_Q\right)$,

then $\gamma_{\min}\left(b_i = b_i\left(p_{I,\min}, p_Q\right)\right) = \gamma\left(p_{I,\min}, p_Q\right)$

};

4. For each bit b_i with $i = 0,1,\cdots,\log_2 M - 1$, perform:

$$\mathrm{LLR}\left(b_i\right) = \gamma_{\min}\left(b_i = 1\right) - \gamma_{\min}\left(b_i = 0\right) \tag{30}$$

■

The proposed algorithm guarantees that the global optimum solution $\left(p_{I,\min}, p_{Q,\min}\right)$ for finding $\min\left\{\left\|\mathbf{y} - \mathbf{hs}\right\|^2\right\}$ is obtained at the end of step 2 after exploring $\sqrt{M}$ integer (constellation) points in signal space. As for the soft bit information *i.e.*, the LLR value, the proposed algorithm allows that these values are obtained, when step 4 is finished after exploring at most (step 2 and step 3 may have overlapped points) $2\sqrt{M}$ integer points. In this way, (6) can be performed without exploring the whole signal space.

B. Architecture Design for Hardware Implementation

The CRML demapper presented in the previous section has not yet been optimized for hardware implementation and needs some further modifications to minimize the amount of required hardware complexity, and to maximize the active time of each hardware component, while respecting the constrains in terms of system throughput.

Since the largest constellation supported by DVB-T2 is 256-QAM with 8 bits per symbol decoded by a LDPC decoder, it is reasonable to assume there are 8 clock cycles between two consecutive QAM symbols for the demapper. Among the different elementary steps, the computations in (11)-(16), (24)-(27) are highly dependent and have a low parallelism degree of 2 processes corresponding to the two components I and Q. Differently from step 1, steps 2 and 3 perform computations for different candidate constellation points and have a high parallelism of $\sqrt{M}$. Finally, step 4 has a $\log_2 M$ level of parallelism since it deals with pure bit-level computations. Therefore the proposed CRML demapper is divided into 3 parts: preprocessing (step 1), computing Euclidean distance metrics (step 2 and step 3), and bit LLRs generation (step 4).

In the preprocessing step, the inversions in (24)-(27) can be implemented by using Newton's method. For any positive number c, its inverse c^{-1} can be calculated iteratively as follows [15]:

$$x^{(n)} = x^{(n-1)}\left(2 - c \cdot x^{(n-1)}\right),\ n = 1,\cdots,N, \tag{31}$$

where n is the iteration index and $\lim_{n\to\infty} x^{(n)} = c^{-1}$. Notice that (31) needs only two multiplications and one subtraction without any division operation.

The accuracy of the inverse value is highly dependent on the iteration number, while the iteration number relies on the initial value $x^{(0)}$. In order to increase computation stability, the fixed point value c is normalized by continuously left-shifting S ($\times 2^S$) or right-shifting S ($\div 2^S$) so that the normalized value $c_0 = 2^S c$ (left-shifted) or $c_0 = 2^{-S} c$ (right-shifted) satisfies $0.5 \le c_0 < 1$. Moreover, in order to reduce the applied number of iterations, the initial value $x^{(0)}$ is set as [16]:

$$x_0^{(0)} = -1.8823 \cdot c_0 + 2.8235. \tag{32}$$

In this way, the approximate reciprocal $x_0^{(n)}$ of c_0 can be obtained by substituting c_0 and $x_0^{(0)}$ into (31), *i.e.*,

$$x_0^{(n)} = x_0^{(n-1)}\left(2 - c_0 \cdot x_0^{(n-1)}\right),\ n = 1,\cdots,N, \tag{33}$$

where $x_0^{(N)}$ is sufficiently accurate after 2 or 3 iterations. Finally, the approximate reciprocal $x^{(N)}$ can be achieved by compensating the factor 2^S:

$$x^{(N)} = \begin{cases} 2^S x_0^{(N)}, & \text{if } c_0 = 2^S c, \\ 2^{-S} x_0^{(N)}, & \text{if } c_0 = 2^{-S} c. \end{cases} \tag{34}$$

During the second step dedicated to compute Euclidean distance metrics for all the candidates, the operation $d_I^2 + d_Q^2$ in (28) and (29) needs 2 multiplications and 1 addition. A possible low-complexity approximation [17] can be provided by:

$$\gamma = d_I^2 + d_Q^2 \approx \left(\max\left(\left|d_I\right|, \left|d_Q\right|\right) + \left(\frac{1}{2} + \frac{1}{16} + \frac{1}{32}\right)\min\left(\left|d_I\right|, \left|d_Q\right|\right)\right)^2. \tag{35}$$

In this way, the 2 multiplications and 1 addition are replaced by 1 multiplication and 3 additions. Since the parallelism in step 2 and step 3 is $\sqrt{M}$, this approximation can save at least $\sqrt{M}$ multipliers.

Therefore, the step for computing Euclidean distance metrics for all the candidates includes the following sub-steps where each sub-step represents 1 system clock cycle:

i. The candidate pairs $\left\{\left(p_I, p_{Q,\min}\right) \mid p_I = 0,1,\cdots,\sqrt{M} - 1\right\}$ and $\left\{\left(p_{I,\min}, p_Q\right) \mid p_Q = 0,1,\cdots,\sqrt{M} - 1\right\}$ are computed by using (23) and (22). The weighted channel attenuation coefficients $\left\{\tilde{h}_{i,j} \cdot p \mid i, j = 1,2 \text{ and } p = 0,1,\cdots,\sqrt{M} - 1\right\}$ can be obtained by only shifting and adding operations in the first clock period;

ii. According to (35), the terms $\left|\tilde{y}_I - \tilde{h}_{1,1} p_{I,\min} - \tilde{h}_{1,2} p_Q\right|$ and $\left|\tilde{y}_Q - \tilde{h}_{2,1} p_{I,\min} - \tilde{h}_{2,2} p_Q\right|$ in (28) are computed. The

min and max of the same $(p_{I,\min}, p_Q)$ pair are then also known;

iii. According to (35), the terms $|\tilde{y}_I - \tilde{h}_{1,1}p_I - \tilde{h}_{1,2}p_{Q,\min}|$, and $|\tilde{y}_Q - \tilde{h}_{2,1}p_I - \tilde{h}_{2,2}p_{Q,\min}|$ in (29) are computed. The min and max of the same $(p_I, p_{Q,\min})$ pair are the known;

iv. Compute the Euclidean distance metrics $\gamma(p_{I,\min}, p_Q)$ for all candidate pairs $(p_{I,\min}, p_Q)$ by using (35);

v. Compute the Euclidean distance metrics $\gamma(p_I, p_{Q,\min})$ for all candidate pairs $(p_I, p_{Q,\min})$ by using (35);

vi. According to the Gray mapping, perform metric comparisons among $\gamma(b_i = b_i(p_I, p_{Q,\min}))$ for all the even indexed bits $i = 0,2,\cdots,\log_2 M - 2$ and find $\gamma_{\min}(b_i = 0)$ and $\gamma_{\min}(b_i = 1)$;

vii. According to Gray mapping, perform metric comparisons among $\gamma(b_i = b_i(p_{I,\min}, p_Q))$ for all the odd indexed bits $i = 1,3,\cdots,\log_2 M - 1$ and find $\gamma_{\min}(b_i = 0)$ and $\gamma_{\min}(b_i = 1)$;

During the step of bit LLR generation, since the maximum number of bits per symbol is 8 (256-QAM), only one LLR $\mathrm{LLR}(b_i)$ is generated within each system clock cycle for each bit b_i by using (30).

C. Computational Complexity Analysis of the Proposed Demapper

In order to simplify the complexity comparison and to get a direct knowledge of the proposed CRML algorithm, a computational complexity analysis is performed in terms of real multiplications (RMs) and real additions (RAs) which are in general the most important metrics for the complexity evaluation. It should be mentioned that a real subtraction is considered as a RA in this paper.

1. (Preprocessing): $\tilde{y}_I$ and $\tilde{y}_Q$ in (11)-(12) need 4 RMs and 2 RAs; $\tilde{h}_{1,1}$, $\tilde{h}_{2,1}$, $\tilde{h}_{1,2}$ and $\tilde{h}_{2,2}$ in (13)-(16) require 8RMs; Since $\tilde{h}_{1,1}\tilde{y}_I$, $\tilde{h}_{2,1}\tilde{y}_Q$, $\tilde{h}_{1,2}\tilde{y}_I$, $\tilde{h}_{2,2}\tilde{y}_Q$, $\tilde{h}_{1,1}\tilde{h}_{1,2}$, $\tilde{h}_{2,1}\tilde{h}_{2,2}$, $\tilde{h}_{1,1}^2$, $\tilde{h}_{2,1}^2$ require 8 RMs, $\tilde{h}_{1,1}\tilde{y}_I + \tilde{h}_{2,1}\tilde{y}_Q$, $\tilde{h}_{1,2}\tilde{y}_I + \tilde{h}_{2,2}\tilde{y}_Q$, $\tilde{h}_{1,1}^2 + \tilde{h}_{2,1}^2$, $\tilde{h}_{1,2}^2 + \tilde{h}_{2,2}^2$, and $\tilde{h}_{1,1}\tilde{h}_{1,2} + \tilde{h}_{2,1}\tilde{h}_{2,2}$ need 5 RAs, and the inversion terms $\frac{1}{\tilde{h}_{1,1}^2 + \tilde{h}_{2,1}^2}$ and $\frac{1}{\tilde{h}_{1,2}^2 + \tilde{h}_{2,2}^2}$ require 8 RMs and 4 RAs by using (33) with 2 iterations. Therefore, the preprocessing step globally needs 28 RMs and 11 RAs.
2. (Computing the Euclidean distance metrics): The computations $\tilde{r}_I + \tilde{c}_Q p_Q$ and $\tilde{r}_Q + \tilde{c}_I p_I$ in (22) and (23) for all the $2\sqrt{M}$ local closest candidate points need $4\sqrt{M} - 2\log_2 M$ RAs; the rounding operations in (22) and (23) for all $2\sqrt{M}$ candidate points require $6\sqrt{M}$ RAs; The computation of Euclidean distance metrics in (35) applies 1 RM and 3 RAs for one distance metric and thus $2\sqrt{M}$ candidate distance metrics require $2\sqrt{M}$ RMs and $6\sqrt{M}$ RAs; moreover, each bit metric $\gamma_{\min}(b_i = b)$ for (30) needs $\sqrt{M}/2 - 1$ RAs and therefore all the distance metrics needs $(\sqrt{M} - 2)\log_2 M$ RAs. Therefore, the computations of the Euclidean distance metrics require $2\sqrt{M}$ RMs and $(\sqrt{M}\log_2 M + 16\sqrt{M} - 4\log_2 M)$ RAs.
3. (Bit LLRs generation): All $\log_2 M$ LLRs by using (30) simply need $\log_2 M$ RAs.

In summary, this algorithm requires a total of $2\sqrt{M} + 28$ RMs, and $\sqrt{M}\log_2 M + 16\sqrt{M} - 3\log_2 M + 11$ RAs for one RCQD constellation symbol.

IV. Logic Synthesis Results and Performance Evaluation

A. Logic Synthesis Results

The general QAM demapper for rotated constellation was synthesized and implemented by using Xilinx ISE. Computational resources of the demapper take up 7637 slice Flip-Flops and 32764 slice LUTs. The corresponding occupation rates are about 3% and (*resp.* 15%) of a Xilinx FPGA 5VLX330FF1760-2 for slice registers (*resp.* slice LUTs). In addition, multiplication resources for the demapper module take up 16 DSP blocks. It represents 8% of the total DSP blocks available in the chosen device. The maximum system clock frequency reaches 96 MHz (the clock period is 10.4 ns) and there are 8 system clocks between two consecutive symbols. So an output LLR rate of 96 MLLR/s for 256-QAM can be achieved at the input I/Q symbol rate of 12 Msymbol/s. Most importantly, only 8 multipliers and 213 adders/subtractors are used.

B. Performance Evaluation and Numerical Computational Complexity Comparisons

The proposed demapping algorithm is compared with other methods in terms of BER and computational complexity, such as the max-log method (see (6)), the MMSE method [8], the sub-region method [9], and the PD-DEM method [13]. In these simulations, perfect synchronization and channel estimation are assumed, which is different from the practical case [18]-[22].

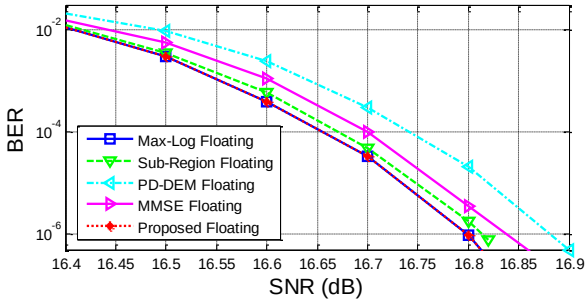

Fig. 1. BER evaluations of floating-point C simulations for DVB-T2 RCQD 256-QAM.

Fig. 1 further compares the floating-point bit error rate (BER) performance of the algorithms in section IV.B. All these methods are evaluated over a Rayleigh fading channel [7] for the RCQD 256-QAM with the 64800-bit long size and 4/5 rate low density parity check (LDPC) channel code defined in the DVB-T2 standard. Without any surprise, the CRML algorithm achieves exactly the same best floating-point performance as the full-complexity max-log

algorithm, since they rely on exactly the same theoretical principles.

TABLE I Complexity Comparison of the considered algorithms for the DVB-T2 RCQD 256-QAM constellation.

Algorithm	CP	RM	RA
Max-Log	256	1032	776
Sub-region	81	332	251
MMSE	16	64	48
PD-DEM	80	390	279
Proposed CRML	32	60	371

TABLE I gives the complexity comparison in terms of candidate point explored (CP), RM and RA to demap the RCQD 256-QAM signal.

It should be mentioned that the low RM number has to be attributed to the equivalent observation model in (10) which greatly simplifies the computation of Euclidean distance metrics. Moreover, although the MMSE demapper seems also attractive over fading channel, it has a very high error floor over fading erasure channel [23],[24].

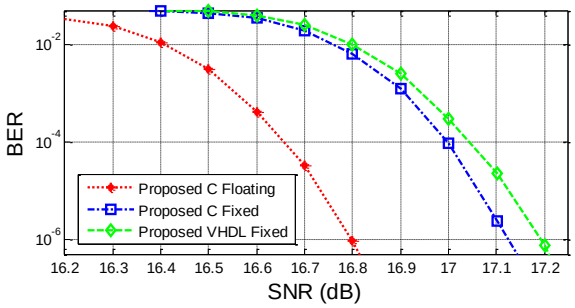

Fig. 2. BER evaluations of the proposed demappers in floating-point C, fixed-point C, and fixed-point hardware simulations for DVB-T2 RCQD 256-QAM.

The C and VHDL fixed-point BER performance of the proposed CRML algorithm is also presented on Fig. 2. In this figure, the C floating-point BER performance of the proposed CRML algorithm serves as reference. It can be observed that there is only a 0.4 dB loss difference between the floating-point version and the VHDL Implemented version including the loss introduced by the hardware of the parallelized LDPC decoder.

V. Conclusion

In this paper, we propose a novel complexity-reduced max-log demapper for RCQD QAM constellations which provides demapping results identical to the full-complexity max-log demapper. The number of operations to obtain hard and soft decisions are reduced to $O\left(\sqrt{M}\right)$. Moreover, a hardware architecture design is detailed with additional simplifications over the original computations. Since the non-rotated constellations are special cases of the rotated ones with rotation angle $\theta = 0$, this proposed demapper can also be applied to the demapping of conventional QAM constellations. Some future work concerns the interface of the proposed scheme with other iterative channel coding [25]-[27].

References

[1] EN 302 755 v1.1.1, Digital Video Broadcasting; Frame structure channel coding and modulation for a second generation digital terrestrial television broadcasting system, ETSI, Sept., 2009.

[2] EN 300 744 v1.6.1, Digital Video Broadcasting; Framing structure, channel coding and modulation for digital terrestrial television, ETSI, Jan. 2009.

[3] C. Abdel Nour and C. Douillard, "Improving BICM performance of QAM constellation for broadcast applications," *in Proc. Int. Symp. on Turbo Codes and Related Topics*, pp. 55-60, Sept. 2008.

[4] C. Douillard and C.A. Nour, "Rotated QAM Constellations to Improve BICM Performance for DVB-T2," *in Proc. of ISSSTA '08.*, pp. 354-359, Aug. 2008.

[5] J.Boutros, and E. Viterbo, "Signal space diversity: a power- and bandwidth-efficient diversity technique for the Rayleigh fading channel," *IEEE Trans. on Info. Theory*, pp.1453-1467, Jul 1998.

[6] X. Giraud, E. Boutillon, and J.C. Belfiore, "Algebraic tools to build modulation schemes for fading channels," *IEEE Trans. on Info. Theory*, vol.43, no.3, pp.938-952, May 1997.

[7] TR 102 831 v1.1.1, Implementation guidelines for a second generation digital terrestrial television broadcasting system (DVB-T2), Oct. 2010.

[8] K. Kim, K. Bae, and H. Yang, "One-Dimensional Soft-Demapping using Decorrelation with Interference Cancellation for Rotated QAM Constellations," *in Proc. IEEE CCNC 2012*, pp. 787-791, Jan. 2012.

[9] M. Li, C. Abdel Nour, C. Jégo, and C. Douillard, "Design of rotated QAM mapper/demapper for the DVB-T2 standard," *in Proc. of IEEE SIPS 2009*, pp. 18-23, Oct. 2009.

[10] M. Li, C. Abdel Nour, C. Jego, and C. Douillard, "Design and FPGA prototyping of a bit-interleaved coded modulation receiver for the DV B-T2 standard," *in Proc. of IEEE SIPS 2010*, pp.162-167, Oct., 2010.

[11] M. Li, C. Abdel Nour, C. Jego, J. Yang, and C. Douillard, "Efficient iterative receiver for bit-Interleaved Coded Modulation according to the DVB-T2 standard," *in Proc. of IEEE ICASSP 2011*, pp. 3168-3171, May 22-27, 2011.

[12] D. Pérez-Calderón, V. Baena-Lecuyer, A. C. Oria, P. López, and J. G.Doblado, "Rotated constellation demapper for DVB-T2," *IEEE Electron. Lett.*, vol. 47, no. 1, pp. 31–32, Jan. 2011.

[13] M. Butussi, and S. Tomasin, "Low Complexity Demapping of Rotated and Cyclic Q Delayed Constellations for DVB-T2," *IEEE Wireless Commun. Lett.*, vol.1, pp.81-84, Apr. 2012.

[14] K. Bae, K. Kim, and H. Yang, "Low complexity two-stage soft demapper for rotated constellation in DVB-T2," *in Proc. of IEEE Intern. Conf. on Consum. Electron.*, pp. 618-619, Jan., 2012.

[15] A. H. Karp, and P. Markstein, "High Precision Division and Square Root," HP Labs Report 93-93-42 (R.1), Oct., 1994.

[16] N. R. Wagner, "Newton's Method to Perform Division," http://www.cs.utsa.edu/~wagner/CS3343/newton/division.html.

[17] J. A. Crawford, "Approximation for RMS," http://www.am1.us/approximation-for-rms/.

[18] S. Bay, B. Geller, A. Renaux, J.P. Barbot, J.M. Brossier, "On the Hybrid Cramér-Rao bound and its Application to Dynamical Phase Estimation", *IEEE Signal Processing letters*, pp. 453-456, vol. 15, 2008.

[19] J. Yang, B. Geller and S. Bay, "Bayesian and Hybrid Cramér-Rao Bounds for the Carrier Recovery under Dynamic Phase Uncertain Channels", *IEEE Trans. on Signal Processing*, pp.667- 680, Feb. 2011.

[20] J. Yang and B. Geller, "Near-optimum Low-Complexity Smoothing Loops for Dynamical Phase Estimation - Application to BPSK modulated signals ", *IEEE Trans. on Signal Processing*, vol. 57, no 9, pp.3704-3711, Sept. 2009.

[21] J. Yang, B. Geller, C. Herzet and J.M. Brossier, "Smoothing PLLs for QAM Dynamical Phase Estimation", *in Proc. of ICC 2009*, June, 2009.

[22] J.M. Brossier, P.O. Amblard, B. Geller, "Self adaptative PLL for general QAM constellations," *in Proc. of EUSIPCO 2002*, pp 631-634, Sept 2002.

[23] J. Yang, K. Wan, B. Geller, C. Abdel Nour, O. Rioul, and C. Douillard, "A Low-Complexity 2D Signal Space Diversity Solution for Future Broadcasting Systems, " *in Proc. of IEEE ICC 2015*, June, 2015.

[24] J. Yang, B. Geller, K. Wan, C. Abdel Nour, O. Rioul, and M. Li, "Uniformly Projected RCQD QAM: A Low-Complexity Signal Space Diversity Solution for Broadcasting Systems and Even More," *IEEE Trans. on Wireless Commun.* (in revision).

[25] C. Vanstraceele, B. Geller, J.P. Barbot, and J.M. Brossier, "Block Turbo Codes for Multicarrier Local Loop Transmission," *in Proc. of IEEE VTC 2002-Fall*, pp. 1773-1775, Oct. 2002.

[26] C. Vanstraceele, B. Geller, J.P. Barbot, and J.M. Brossier, "A Low Complexity Block Turbo Decoder Architecture," *IEEE Trans. on Commun.*, vol. 56, no 12, pp. 1985-1989, Dec. 2008.

[27] B. Geller, I. Diatta, J.P. Barbot, C. Vanstraceele, and F. Rambeau, "Block Turbo Codes: From Architecture to Application," *in Proc. of IEEE Int. Symp. on Info. Theory, ISIT 2006*, July 2006.